

Bounds on the energy of a soft cubic ferromagnet with large magnetostriction

Raghavendra Venkatraman ^{*1}, Vivekanand Dabade ^{†2}, and Richard D. James ^{‡3}

¹*Department of Mathematical Sciences, Carnegie Mellon University, Pittsburgh PA.*

²*LMS, École Polytechnique, CNRS, Université Paris-Saclay, Palaiseau 91128, France*

³*Aerospace Engineering and Mechanics Department, University of Minnesota, Minneapolis, MN.*

July 19, 2022

Dedicated to Peter Sternberg on the occasion of his sixtieth birthday, with respect and admiration.

Abstract: We complete the analysis initiated in [5] on the micromagnetics of cubic ferromagnets in which the role of magnetostriction is significant. We prove ansatz-free lower bounds for the scaling of the total micromagnetic energy including magnetostriction contribution, for a two-dimensional sample. This corresponds to the micromagnetic energy-per-unit-length of an infinitely thick sample. A consequence of our analysis is an explanation of the multi-scale zig-zag Landau state patterns recently reported in single crystal Galfenol disks from an energetic viewpoint. A second corollary of our analysis is a variational justification of the branched microstructure seen in Iron; this answers a question raised by Choksi, Kohn and Otto in [3]. Our proofs use a number of well-developed techniques in energy-driven pattern formation, along with the use of tools from Fourier analysis for the magnetostriction term.

1 Introduction and setup of the problem

We are interested in deriving optimal energy scaling laws for a ferromagnetic sample with cubic anisotropy. Important examples of cubic ferromagnets include Iron [14],

^{*}rvenkatr@andrew.cmu.edu

[†]vivekanand.dabade@polytechnique.edu

[‡]james@umn.edu

Permalloy [8], Tefenol-D [6], and Galfenol [4]. These ferromagnets, when magnetized, undergo spontaneous elastic deformation; this is known as magnetostriction. Iron and Permalloy are low magnetostrictive materials, whereas Terfenol-D and Galfenol are large magnetostrictive materials. Materials with large magnetostriction exhibit a fascinating interplay of elasticity and magnetism. Inspired by recent experiments on Galfenol reported in [4], we initiated a variational study of cubic ferromagnets with magnetostriction in [5]. In [5], we first analyzed Young measures arising as limits of minimizing sequences for the so-called no-exchange relaxation and applied this analysis to derive macroscopic properties of Galfenol. Restoring the exchange energy term, defined below, we then derived rigorous upper bounds for the scaling of the optimal energy for the full micromagnetic energy functional in the presence of magnetostriction. Our upper bounds required fairly complex multi-scale constructions inspired by the micrographs in [4]. The goal of the present paper is to supplement this upper bound with an ansatz-free lower bound, within a two dimensional setting that is motivated by the geometry of the sample in [4]. This lower bound demonstrates that within the parameter regime of Galfenol, one can not do energetically better than our constructions from [5].

Towards describing the functional that is at the core of our paper, we first set some notation. We let $G \subset \mathbb{R}^2$ denote the unit cube $\left(-\frac{1}{2}, \frac{1}{2}\right)^2$. We define the functions $\varphi : \mathbb{R}^2 \rightarrow \mathbb{R}$ and $\epsilon_0 : \mathbb{R}^2 \rightarrow \mathbb{R}^{2 \times 2}$ by the formulas

$$\varphi(z) = \varphi(z_1, z_2) := (z_1^2 - z_2^2)^2, \quad (1.1)$$

$$\epsilon_0(z) = z \otimes z - \frac{1}{2} I_2 = \begin{pmatrix} z_1^2 & z_1 z_2 \\ z_2 z_1 & z_2^2 \end{pmatrix} - \frac{1}{2} \begin{pmatrix} 1 & 0 \\ 0 & 1 \end{pmatrix}. \quad (1.2)$$

Finally, for a function $u \in H^1(G; \mathbb{R}^2)$, we define

$$\epsilon(u) := \frac{\nabla u + (\nabla u)^T}{2}. \quad (1.3)$$

Let $v \in H^1(G; \mathbb{R}^2)$ and let \tilde{v} denote the extension of v to \mathbb{R}^2 by zero outside of G . For fixed positive numbers μ, β we consider the sequence of (*fully non-dimensionalized*) variational problems indexed by $\eta > 0$ that will be the subject of this paper, given by

$$\begin{aligned} \mathcal{F}_\eta(v) = \mu\eta \int_G |\nabla v|^2 d\mathbf{x} + \frac{\mu}{\eta} \int_G \left((|v|^2 - 1)^2 + \varphi(v) \right) d\mathbf{x} + \beta \|\operatorname{div} \tilde{v}\|_{H^{-1}(\mathbb{R}^2)}^2 \\ + \inf_{u \in H^1(G; \mathbb{R}^2)} \int_G \|\epsilon(u) - \epsilon_0(v)\|^2 d\mathbf{x}, \end{aligned} \quad (1.4)$$

where $\beta > 0$. The motivation for this scaling and the derivation of this model will be made clear in Sec. 1.1 below; for now, let us simply remark that in this scaling, the energies $\mathcal{F}_\eta(v)$ are bounded as $\eta \rightarrow 0$. Our main theorem is

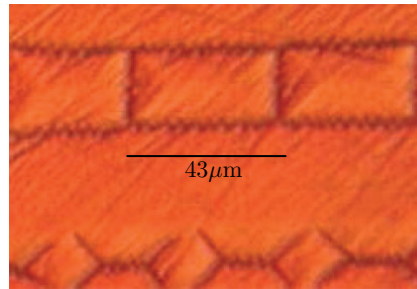
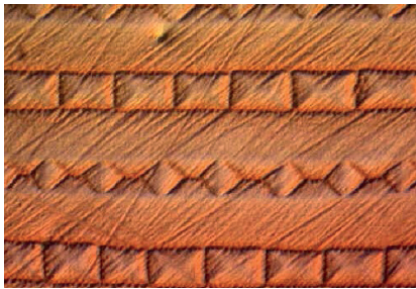
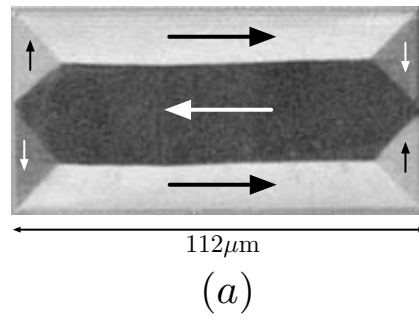


Figure 1: Experimental Micrographs. (a) Normal Landau state seen in Permalloy, [11]. (b) and (c) Zig-zag Landau state seen in Galfenol, [4].

Theorem 1.1. *There exists universal constants $0 < c_1 < 1, c_2, c_3 > 0$ such that the following holds: for any $\mu \in (0, c_1)$, and $\beta < c_2$, we have*

$$\frac{1}{c_3} \mu^{2/3} \beta^{1/3} \geq \liminf_{\eta \rightarrow 0} \inf_{v \in H^1(G; \mathbb{R}^2)} \mathcal{F}_\eta(v) \geq c_3 \mu^{2/3} \beta^{1/3}. \quad (1.5)$$

Remark 1.2. *The constants appearing in the statement of the theorem are universal; we have not made an effort to optimize them.*

The proof of the upper bound inequality is essentially contained in [5], and is recalled briefly in Section 3. In that section, we also recall other constructions detailed in [2] that are based on domain branching. The proof of the lower bound inequality is the content of Section 4. The rest of this introduction is devoted to deriving the energy (1.4) from the micromagnetic functional.

1.1 Derivation of the energy (1.4) from micromagnetics

Geometry and motivation for the two-dimensional reduction:

The geometry of the sample we have in mind is cylindrical with axis along the z -axis, whose characteristic dimension L in the $x-y$ plane is significantly smaller than its thickness along the z -axis. This geometry is motivated by experimental values of $L \sim 10^{-5}m$ and sample thickness along the z -axis $\sim 10^{-3}m$; see Extended Data Figure 4 in [4]. It permits us to work with a two-dimensional energy, that we think of as the energy per unit length of an infinitely long sample; we however do not attempt to derive this energy from the full three-dimensional model via a rigorous limiting procedure. The two-dimensional nature of our model is, however, crucial to our analysis of the magnetostriction and the magnetostatic energies. Indeed, the analysis of the magnetostriction energy relies on the Fourier analysis of a certain nonlinear function of the magnetization: this is made tractable by the nonconvex constraint that the magnetization is S^1 -valued, yielding (somewhat surprising) cancellations. We point out that the micrographs for Galfenol, which were the original motivation of our project, have essentially in-plane magnetization. Furthermore, our two-dimensional constructions in [5] accurately predict the (macroscopic) average strain as measured in experiments on Galfenol.

Setup from micromagnetics

Let $\Omega \subset \mathbb{R}^2$ denote an open bounded domain that represents the cross-section of the ferromagnetic sample. Within the variational theory of micromagnetics, the magnetization

of the sample is described by a vector field $\mathbf{m} : \Omega \rightarrow \mathbb{R}^3$ that satisfies $|\mathbf{m}| = 1$ almost everywhere in Ω . The magnetization \mathbf{m} is extended by zero outside of Ω . With an eye of working within a two-dimensional theory, we limit ourselves to competitors of the form $\mathbf{m}(x, y) = (m_1(x, y), m_2(x, y), 0)$. Our starting point towards formally deriving (1.4) is the full micromagnetic energy including magnetostriction, and in the absence of an external magnetic field, given by

$$\mathbb{F}(\mathbf{m}) = \underbrace{A \int_{\Omega} |\nabla \mathbf{m}|^2 d\mathbf{x}}_{\text{wall energy}} + \underbrace{K_a \int_{\Omega} \varphi(\mathbf{m}) d\mathbf{x}}_{\text{anisotropy energy}} + \underbrace{c_{44} \lambda_{111}^2 \tilde{e}_{\text{mag}}(\mathbf{m})}_{\text{magnetostriction energy}} + \underbrace{K_d \int_{\mathbb{R}^2} |\mathbf{h}_m|^2 d\mathbf{x}}_{\text{magnetostatic energy}}. \quad (1.6)$$

$$\text{where } \tilde{e}_{\text{mag}}(\mathbf{m}) = \inf_{\tilde{\mathbf{E}}(\mathbf{u}) \text{ compatible}} \int_{\Omega} (\tilde{\mathbf{E}}(\mathbf{u}) - \tilde{\mathbf{E}}_0(\mathbf{m})) \cdot \tilde{\mathbb{C}}(\tilde{\mathbf{E}}(\mathbf{u}) - \tilde{\mathbf{E}}_0(\mathbf{m})) d\mathbf{x}. \quad (1.7)$$

Here, $A, K_a, c_{44}, \mathbb{C}, K_d, c_{44} \lambda_{111}^2$ are all material parameters that we describe below. The magnetostriction energy defined in (1.7) corresponds to the least linear elastic energy associated to a preferred non-dimensional strain tensor $\tilde{\mathbf{E}}_0(\mathbf{m})$. The last term in the energy (1.6) is the magnetostatic energy associated to a magnetization \mathbf{m} : it is derived from Maxwell's equations, and in short, penalizes the divergence of the field \mathbf{m} in a negative Sobolev norm. We will explain both these energies in greater detail in the paragraphs to come. We point out that in our formulation above, the total micromagnetic energy $\mathbb{F}(\mathbf{m})$ represents the three-dimensional energy per unit length along the z -direction and has dimensions [energy/length].

Exchange and magnetocrystalline anisotropy energies

The *exchange constant* is denoted by A and typically satisfies $0 < A \ll 1$. In the literature on energy-driven pattern formation, it is also common (see [2, 3, 5]) to use the so-called sharp interface functional, in which the exchange energy is measured by the BV semi-norm \mathbf{m} of the magnetization \mathbf{m} as opposed to the Dirichlet energy as in (1.6). Thus, in these studies, one might see an expression of the form

$$\mu \int_{\Omega} |\nabla \mathbf{m}|, \quad (1.8)$$

where $\mu > 0$ is the *wall cost* per unit length. Before discussing how the sharp interface and diffuse energies are related, we discuss the magnetocrystalline anisotropy energy.

The magnetocrystalline anisotropy energy, or simply anisotropy, sets certain crystallographic directions, referred to as the *easy axes*, energetically preferred for the magnetization \mathbf{m} . The *anisotropy energy density* ($K_a \varphi(\mathbf{m})$) is determined by the anisotropy

energy coefficient $K_a > 0$ ¹ and $\varphi(\mathbf{m})$ given by

$$\varphi(\mathbf{m}) = \left(\frac{1}{4} - m_1^2 m_2^2 \right) = \frac{1}{4} (m_1^2 - m_2^2)^2. \quad (1.9)$$

The wells of the anisotropy energy are referred to as the *easy axes* of the sample, and in our case are given by $\pm \mathbf{m}_1, \pm \mathbf{m}_2$, where $\mathbf{m}_1 = (1/\sqrt{2}, 1/\sqrt{2}, 0)$ and $\mathbf{m}_2 = (1/\sqrt{2}, -1/\sqrt{2}, 0)$.

How are the sharp-interface version of the exchange energy, (1.8) and the diffuse counterpart in (1.6) related? To answer this question, it is helpful to record the dimensions of the various quantities in question. Since our functional \mathbb{F} from (1.6) has dimensions of energy per unit length (in the z -direction), one has

$$[A] = \frac{[\text{Energy}]}{[\text{Length}]}, \quad [K_a] = \frac{[\text{Energy}]}{[\text{Length}]^3} \quad [\gamma] = \frac{[\text{Energy}]}{[\text{Length}]^2}. \quad (1.10)$$

For sufficiently large values of the anisotropy constant $|K_a|$, the magnetization \mathbf{m} stays close to the easy axes of the sample, thus being essentially piecewise constant and forming *magnetic domains*. Different domains are separated by thin transition layers. Competition between the diffuse exchange energy $A \int |\nabla \mathbf{m}|^2$ and the anisotropy energy $\int K_a \varphi(\mathbf{m})$ sets a *surface tension* μ that effectively penalizes the *surface area of the transition layer* $\int |\nabla \mathbf{m}|$. The width of a transition layer must necessarily be smaller than the characteristic length L , which yields

$$\sqrt{\frac{A}{K_a}} < L. \quad (1.11)$$

Under these circumstances, one can show that the surface tension is related to the exchange constant A by

$$\mu^2 \sim A K_a. \quad (1.12)$$

From the point of view of optimal energy scaling laws, these two formulations are asymptotically equivalent due to the Modica-Mortola inequality, see [7, Section 6.8]. The sharp-interface formulation has certain advantages: it permits one to focus attention on the domain morphology without having to simultaneously resolve the internal structure of walls. It is the sharp-interface formulation that we used in [5], because this simplified our computations concerning the upper bound. The rigorous connection between the sharp interface and diffuse formulations is conveniently done using Γ -convergence; see [19], also [7, Section 6.8]. The diffuse formulation naturally has an extra small

¹Our choice of signs here is a bit different from convention: the materials that are of interest in this paper are “negative anisotropy materials”, with $K_a < 0$ and correspondingly φ is defined by the negative of Eq. (1.9), nevertheless rendering the product $K_a \varphi$ nonnegative.

length-scale $\eta > 0$ corresponding to the diffuse wall thickness, as compared to the sharp interface limit. The $\eta \rightarrow 0$ limiting procedure yielding the sharp interface limit can then be made precise in the parameter regime $A \sim \mu\eta$, $K_a \sim \frac{\mu}{\eta}$, consistent with (1.12).

While the magnetization \mathbf{m} is S^1 -valued and the diffuse exchange energy which is present in the full micromagnetic energy (1.6) penalizes the H^1 -seminorm of \mathbf{m} , it is well known [1] that S^1 -valued vector fields in the plane having vortices have infinite H^1 -seminorm. However, even the normal Landau state, refer to Figure 1 (a) has vortices, at each triple junction.

A convenient “remedy” to this issue is to relax the “hard” constraint $|\mathbf{m}| = 1$, and replace \mathbf{m} by a vector field $\mathbf{v} : \Omega \rightarrow \mathbb{R}^2$ along with a penalty term in the energy which forces \mathbf{v} to be nearly S^1 -valued; see again [1]. This corresponds to the term Ginzburg-Landau term $\frac{\mu}{\eta} \int_G (|\mathbf{v}|^2 - 1)^2 d\mathbf{x}$ in the energy (1.4), where η is a non-dimensional version of η that will be explained below. In this scaling, the cost of a vortex is $\eta |\log \eta|$ which vanishes in the $\eta \rightarrow 0^+$ limit considered in Theorem 1.1.

While the Ginzburg-Landau penalty might seem like a mathematical artefact, it can be physically thought of as penalizing out-of-plane magnetization, and the walls correspondingly as Bloch walls. Since we wish to work with a two-dimensional theory, we do not pursue this interpretation; the reader might wish to see [10] for instance.

Magnetostriction energy.

We next turn to the *magnetostriction energy*, the third term in (1.6). Our reference for modeling this energy is [12] which relies on linear elasticity. For notational consistency with [12], and for the convenience of the reader, we briefly describe full three-dimensional magnetostriction. Subsequently, we describe our two-dimensional reduction. The preferred strain associated to a magnetization $\mathbf{m} = (m_1, m_2, m_3) : \Omega \rightarrow \mathbb{S}^2$ is given by

$$\mathbf{E}_0(\mathbf{m}) = \frac{3}{2} \left(\lambda_{100} (\mathbf{m} \otimes \mathbf{m} - \frac{1}{3} \mathbf{I}) + (\lambda_{111} - \lambda_{100}) \sum_{i \neq j} m_i m_j \mathbf{e}_i \otimes \mathbf{e}_j \right), \quad (1.13)$$

where the vectors $\{\mathbf{e}_1, \mathbf{e}_2, \mathbf{e}_3\}$ in (1.13) refer to an orthonormal basis parallel to the cubic axes. The constants λ_{100} and λ_{111} are referred to as the magnetostriction constants of the cubic material. The elastic energy associated to a magnetization \mathbf{m} and a displacement $\mathbf{u} \in H^1(\Omega; \mathbb{R}^3)$ is given by

$$\frac{1}{2} \int_{\Omega} (\mathbf{E}(\mathbf{u}) - \mathbf{E}_0(\mathbf{m})) : \mathbb{C} (\mathbf{E}(\mathbf{u}) - \mathbf{E}_0(\mathbf{m})) d\mathbf{x}, \quad \mathbf{E}(\mathbf{u}) = \frac{\nabla \mathbf{u} + \nabla \mathbf{u}^T}{2}.$$

In the above, \mathbb{C} is a fourth order, positive-definite, symmetric tensor, referred to as the elastic modulus. For a cubic material such as Galfenol, the elastic modulus \mathbb{C} consists of 3 independent components, c_{11}, c_{12} and c_{44} . Minimizing the elastic energy over all mechanically compatible strains, i.e. all strains \mathbf{E} that arise as a symmetric gradient of an H^1 -displacement field \mathbf{u} results in (1.7). For a brief discussion on the role of mechanical compatibility in our variational problem, we refer the reader to [5].

With this background on magnetostriction, we turn to making simplifications that result in a two-dimensional theory that we use in our analysis. First, for Galfenol, one has $c_{11} \approx c_{12} \approx c_{44} \approx 10^{11} \text{ N/m}^2$, refer to [20]. We will therefore only use one elastic constant, namely c_{44} and set

$$c_{11} = c_{12} = c_{44}. \quad (1.14)$$

Furthermore, as for the magnetostriction constants, refer to [5] and references therein, one has $\lambda_{100} \approx \lambda_{111} \approx 10^{-4}$. Consequently, we set

$$\lambda_{100} = \lambda_{111}. \quad (1.15)$$

With these assumptions, the preferred strain simplifies to

$$\mathbf{E}_0(\mathbf{m}) = \frac{3\lambda_{111}}{2} \left((\mathbf{m} \otimes \mathbf{m} - \frac{1}{3}\mathbf{I}) \right). \quad (1.16)$$

Second, we note that in our two-dimensional framework, since \mathbf{m} is in-plane, i.e. \mathbf{m} takes the form $(m_1(x, y), m_2(x, y))$ and $m_3 = 0$, the preferred strain reduces to

$$\mathbf{E}_0(\mathbf{m}) = \frac{3\lambda_{111}}{2} \begin{pmatrix} m_1^2 - \frac{1}{3} & m_1 m_2 & 0 \\ m_1 m_2 & m_2^2 - \frac{1}{3} & 0 \\ 0 & 0 & -\frac{1}{3} \end{pmatrix}.$$

Motivated by the micrographs in [4], a more significant restriction that we make is to look at displacements of the form

$$\mathbf{u}(x, y, z) = \left(u_1(x, y), u_2(x, y), \frac{-\lambda_{111}}{2} z \right) \quad (1.17)$$

With this choice, the actual strain is given by

$$\mathbf{E}(\mathbf{u}) = \begin{pmatrix} \frac{\partial u_1}{\partial x} & \frac{1}{2} \left(\frac{\partial u_1}{\partial y} + \frac{\partial u_2}{\partial x} \right) & 0 \\ \frac{1}{2} \left(\frac{\partial u_1}{\partial y} + \frac{\partial u_2}{\partial x} \right) & \frac{\partial u_2}{\partial y} & 0 \\ 0 & 0 & -\frac{\lambda_{111}}{2} \end{pmatrix}.$$

It is thus clear that we can identify \mathbf{u} with a vector in \mathbb{R}^2 of the form $\mathbf{u}(x, y) = (u_1(x, y), u_2(x, y))$, and correspondingly identify the actual and preferred strains with their top-left 2×2 blocks, viz.

$$\bar{\epsilon}_0(\mathbf{m}) = \frac{3\lambda_{111}}{2} \left(\mathbf{m} \otimes \mathbf{m} - \frac{1}{3} I_2 \right) = \frac{3\lambda_{111}}{2} \begin{pmatrix} m_1^2 - \frac{1}{3} & m_1 m_2 \\ m_1 m_2 & m_2^2 - \frac{1}{3} \end{pmatrix}, \quad (1.18)$$

$$\bar{\epsilon}(\mathbf{u}) = \begin{pmatrix} \frac{\partial u_1}{\partial x} & \frac{1}{2} \left(\frac{\partial u_1}{\partial y} + \frac{\partial u_2}{\partial x} \right) \\ \frac{1}{2} \left(\frac{\partial u_1}{\partial y} + \frac{\partial u_2}{\partial x} \right) & \frac{\partial u_2}{\partial y} \end{pmatrix}. \quad (1.19)$$

As our third simplification, we note that the constraint $m_1^2 + m_2^2 = 1$ renders the tensor $\bar{\epsilon}_0(\mathbf{m})$ to have trace $\frac{\lambda_{111}}{2}$. For simplicity in our estimates, it is desirable to have the preferred strain be trace-free. We therefore define

$$\bar{\bar{\epsilon}}_0(\mathbf{m}) = \bar{\epsilon}_0(\mathbf{m}) - \frac{\lambda_{111}}{2} I_2, \quad \bar{\bar{\epsilon}}(\mathbf{u}) = \bar{\epsilon}(\mathbf{u}) - \frac{\lambda_{111}}{2} I_2, \quad (1.20)$$

where I_2 is the identity matrix in \mathbb{R}^2 . Obviously, this does not change the elastic energy associated to a magnetization \mathbf{m} and a corresponding displacement \mathbf{u} of the form (1.17).

Our last simplification is one of non-dimensionalization: we set

$$\tilde{\mathbb{C}} = \frac{\mathbb{C}}{c_{44}}, \quad \epsilon_0(\mathbf{m}) = \frac{\bar{\bar{\epsilon}}_0(\mathbf{m})}{\lambda_{111}}, \quad \epsilon(\mathbf{u}) = \frac{\bar{\bar{\epsilon}}(\mathbf{u})}{\lambda_{111}}. \quad (1.21)$$

Putting together (1.14), (1.15), (1.20) and (1.21) we find the magnetostriction energy from equation (1.7) associated to a magnetization \mathbf{m} is given by

$$\inf_{\mathbf{u} \in H^1(\Omega; \mathbb{R}^2)} c_{44} \lambda_{111}^2 \int_{\Omega} \|\epsilon(\mathbf{u}) - \epsilon_0(\mathbf{m})\|^2 d\mathbf{x} \quad (1.22)$$

with $\|A\|^2$ denoting the sum of the square of the entries of the matrix A . We will denote the magnetostriction energy coefficient as $c_{44} \lambda_{111}^2$.

Magnetostatic energy.

The final term in our energy is the *magnetostatic energy* and the relevant material parameter is known as magnetostatic energy coefficient K_d . The magnetostatic energy penalizes the induced or stray field \mathbf{h}_m associated to the magnetization \mathbf{m} . The induced field \mathbf{h}_m is obtained by solving Maxwell's equations of magnetostatics on \mathbb{R}^2 ,

$$\nabla \cdot (\mathbf{h}_m + \mathbf{m}) = 0, \quad (1.23a)$$

$$\nabla \times \mathbf{h}_m = 0. \quad (1.23b)$$

in $H^{-1}(\mathbb{R}^2)$. We remind the reader that since our sample is infinitely thick in the z -direction, the magnetostatic energy in (1.6) is interpreted as the magnetostatic energy per unit length of the sample in the z -direction. It is then easily seen that

$$\int_{\mathbb{R}^2} |\mathbf{h}_m|^2 d\mathbf{x} = \|\operatorname{div} \mathbf{m}\|_{H^{-1}(\mathbb{R}^2)}^2.$$

Parameter regime and derivation of the functional (1.4)

A primary motivation for our project is the fascinating two-scale microstructure in Galfenol [4]; the authors there refer to this pattern as the *zig-zag Landau state*. The magnetic microstructure in Galfenol is in striking contrast to known traditional soft ferromagnets such as Permalloy, that exhibit the so-called “*normal Landau state*” refer to Figure 1. Our point of view in [5] and the present paper is to explain this complex microstructure as the result of the competition between magnetostriction energy, which prefers high frequency oscillations in the magnetization, and the small yet nonzero wall energy, which favors relatively few domain walls. Indeed, the magnetostrictive strains in Galfenol ($\approx 10^{-4}$) are much larger than traditional ferromagnets ($\approx 10^{-6}$). Furthermore, the large magnetostriction energy coefficient in Galfenol is comparable to the anisotropy energy coefficient, i.e. $c_{44}\lambda_{111}^2 \approx K_a \approx 10^3$. In contrast, in Permalloy, the magnetostriction energy coefficient is much smaller than the anisotropy energy coefficient, i.e. $c_{44}\lambda_{111}^2 \approx 10^{-1} \ll K_a \approx 10^2$.

In [5] we constructed an upper bound for the micromagnetic energy based on a zig-zag Landau state construction. The construction reported there was an interpretation of the micrographs from [4]. The goal of our paper is to prove a matching ansatz-free lower bound. For clarity, we work with in a parameter regime of a soft ferromagnet in which magnetostriction is strongly coupled with anisotropy. Furthermore, we suppose that the sample cross-section is given by the square

$$\Omega = \left(-\frac{L}{2}, \frac{L}{2}\right)^2.$$

Rescaling the domain by the characteristic length L , we arrive at a functional defined on the unit square

$$G := \left(-\frac{1}{2}, \frac{1}{2}\right)^2.$$

Non-dimensionalizing the energy by dividing through by $c_{44}\lambda_{111}^2 L^2$, and defining the

(non-dimensional) positive numbers μ, η, Q_η via

$$\begin{aligned}\mathcal{F}_\eta(v) &:= \frac{1}{c_{44}\lambda_{111}^2 L^2} \mathbb{R}(v), & \mu\eta &:= \frac{A}{c_{44}\lambda_{111}^2 L^2}, \\ \frac{\mu}{\eta} &:= \frac{K_a}{c_{44}\lambda_{111}^2}, & \beta &= \frac{K_d}{c_{44}\lambda_{111}^2},\end{aligned}$$

we arrive at the energy (1.4). Here, μ plays the role of a non-dimensional surface tension, refer to (1.12), and η a non-dimensional diffuse wall-thickness.

2 Preliminaries

2.1 Fourier analysis

We will make crucial use of Fourier Analysis, specifically in our analysis of the magnetostriction energy and its lower bound. We set some notation in this section and collect a number of results for the convenience of the reader. This section is mainly drawn from [18].

Let $f \in L^1(\mathbb{R}^n)$. Recall that the Fourier transform of the function f is defined by letting

$$\hat{f}(\xi) = \int_{\mathbb{R}^n} f(\mathbf{x}) e^{-2\pi i \xi \cdot \mathbf{x}} d\mathbf{x}, \quad (2.1)$$

with \cdot denoting the usual (Euclidean) inner product. We crucially use L. Schwartz's version of the Paley-Wiener theorem which concerns Fourier transforms of distributions with compact support. This is natural in our context, since the magnetization is supported in the (closure of the) sample domain. To state Schwartz's version of the Paley-Wiener theorem, recall that in (2.1), allowing ξ to vary over \mathbb{C}^n as opposed to \mathbb{R}^n results in the so-called Fourier-Laplace transform. Schwartz's version of the Paley-Wiener theorem asserts that an entire function F on \mathbb{C}^n is the Fourier-Laplace transform of a distribution v with compact support if and only if for all $z \in \mathbb{C}^n$, one has the bounds

$$|F(z)| \leq C(1 + |z|)^N e^{B \operatorname{Im}(z)},$$

for some constants C, N, B . Entire functions satisfying such an estimate are said to be of exponential type B . A posteriori, the distribution v is in fact supported in the closed ball centered at the origin of radius B . The crucial Plancherel-Polya inequality [16] implies that if F is an entire function of exponential type B , and if its restriction \hat{f} to \mathbb{R}^n

belongs to $L^p(\mathbb{R}^n)$ for some $p \in [1, \infty)$, then one has ²

$$\sum_{\mathbf{k} \in \mathbb{Z}^n} |F(\mathbf{k})|^p \sim \|F\|_{L^p(\mathbb{R}^n)}^p. \quad (2.2)$$

Here, we identify $\mathbb{R}^n \subset \mathbb{C}^n$ as the real parts of the frequencies $\xi \in \mathbb{C}^n$. We refer the reader to [16] for related discussion, but briefly summarize the idea behind this estimate. The proof of this estimate relies on the fact that the function $[0, \infty) \ni t \mapsto t^p$ being strictly increasing and convex, and $z \mapsto F(z)$ being analytic, the map $z \mapsto |F(z)|^p$ is pluri-subharmonic. Given a well-spaced set of discrete points such as the integers, one can thus use the sub-averaging of pluri-subharmonic functions along with L^p estimates on the Fourier transform to obtain the summability estimate (2.2).

To specialize these results to the setting that we will use them in, let G denote the unit cube in \mathbb{R}^2 , i.e. $G = \left(-\frac{1}{2}, \frac{1}{2}\right)^2$. For any $f \in L^2(\mathbb{R}^2)$, one defines the Fourier transform of f by

$$\hat{f}(\xi) := \lim_{R \rightarrow \infty} \int_{(-R, R)^2} f(\mathbf{x}) e^{-i2\pi \xi \cdot \mathbf{x}} d\mathbf{x} \quad \xi \in \mathbb{R}^2,$$

where the limit is taken in the L^2 -sense. If in addition, f is supported in G , then its Fourier transform \hat{f} is the restriction to \mathbb{R}^2 of the entire function F on \mathbb{C}^2 defined by

$$F(\mathbf{z}) = \int_G f(\mathbf{x}) e^{-2\pi i \mathbf{x} \cdot \mathbf{z}} d\mathbf{x}, \quad (2.3)$$

where we define $x \cdot z = x_1 z_1 + x_2 z_2$. By the Plancherel-Polya inequality, there exists a constant $C > 0$ such that

$$\sum_{\mathbf{k} \in \mathbb{Z}^2} |F(\mathbf{k})|^2 \leq C \int_{\mathbb{R}^2} |F(\mathbf{x})|^2 d\mathbf{x}. \quad (2.4)$$

This in particular yields that the sequence $\{F(\mathbf{k})\}_{\mathbf{k} \in \mathbb{Z}^2}$ is square-summable. We point out that $\{F(k)\}$ is precisely the sequence of Fourier coefficients thinking of f as a 1-periodic function. In particular, the Fourier transform F satisfies

$$f(\mathbf{x}) = \sum_{\mathbf{k} \in \mathbb{Z}^2} F(\mathbf{k}) e^{2\pi i \mathbf{k} \cdot \mathbf{x}}$$

as functions in $L^2(G)$. Finally, we in fact have the *equality*

$$\int_G |f(\mathbf{x})|^2 d\mathbf{x} = \sum_{\mathbf{k} \in \mathbb{Z}^2} |F(\mathbf{k})|^2. \quad (2.5)$$

²Notation: By $A \sim B$ we mean that there exist universal constants c and $C > 0$ such that $cA \leq B \leq CA$.

2.2 On the magnetostriction energy

We recall the following version of Korn's inequality (refer to [15]) that we will use to show that for any magnetization \mathbf{m} , one has a displacement \mathbf{u} that achieves the infimum in (1.22).

Theorem 2.1. *Let $\Omega \subset \mathbb{R}^n$ denote a bounded, open set with Lipschitz boundary. There exists a constant $C(n, \Omega)$ such that*

$$\|\nabla u\|_{H^1(\Omega)} \leq C \left\| \frac{\nabla u + \nabla u^T}{2} \right\|_{L^2(\Omega)}, \quad (2.6)$$

for all $u \in H^1(\Omega; \mathbb{R}^n)$ such that

- (i) for $i \in \{1, \dots, n\}$, we have $\int_{\Omega} u_i \, d\mathbf{x} = 0$,
- (ii) the matrix $a_{ij} := \left[\int_{\Omega} \nabla_i u^j \, d\mathbf{x} \right]$ is symmetric.

Using this theorem, concerning the variational problem in (1.22) we prove

Theorem 2.2. *Let $\mathbf{m} \in L^2(\Omega)$. Then there exists $\mathbf{u}_0 \in H^1(\Omega)$ with $\int_{\Omega} \mathbf{u}_0^i \, d\mathbf{x} = 0$ and $\int_{\Omega} \nabla_i \mathbf{u}_0^j \, d\mathbf{x} = 0$ for every $i, j \in \{1, \dots, N\}$, such that*

$$\int_{\Omega} \|\epsilon(\mathbf{u}_0) - \epsilon_0(\mathbf{m})\|^2 \, d\mathbf{x} = \inf_{\mathbf{u} \in H^1(\Omega; \mathbb{R}^2)} \|\epsilon(\mathbf{u}) - \epsilon_0(\mathbf{m})\|^2 \, d\mathbf{x} \quad (2.7)$$

Proof. The proof is an easy application of the direct method in the Calculus of Variations, and we outline it. For ease of notation, set $V := e_0(\mathbf{m})$ and note that $\|V\|_{L^2(\Omega)} \leq C$. Let $\{\mathbf{u}_j\} \subset H^1(\Omega; \mathbb{R}^2)$ denote a minimizing sequence for the variational problem in (2.7). Since the energy on the right hand side of (2.7) does not change upon adding constants and infinitesimal rotations, we may assume that for each $j \in \mathbb{N}$, one can

- (i) add an appropriate constant to each \mathbf{u}_j to arrange $\int_{\Omega} (\mathbf{u}_j)_i \, d\mathbf{x} = 0$, for $i \in \{1, \dots, N\}$,
- (ii) add an appropriate infinitesimal rotation $W_j \mathbf{x}$ to \mathbf{u}_j , with W_j skew symmetric, so that for each $j \in \mathbb{N}$, we can arrange that the matrix $c_{ik}^j := \left[\int_{\Omega} \nabla_i (\mathbf{u}_j)^k \, d\mathbf{x} \right]$ is symmetric: that is $c_{ik}^j = c_{ki}^j$ for each $j \in \mathbb{N}$, and for all $i, k \in \{1, 2\}$.

These operations do not change the energy in (2.7) of the functions \mathbf{u}_j . Denoting by m the inf on the right hand side of (2.7), one easily obtains by Korn's inequality, refer to Theorem 2.1 that for all j sufficiently large,

$$\|\mathbf{u}_j\|_{H^1(\Omega)}^2 \leq C \left(\|\epsilon(\mathbf{u}_j) - V\|^2 + 1 \right) \leq C(m + 2).$$

The result follows by usual compactness and weak-lower semicontinuity theorems. \square

In the next lemma, we obtain a Fourier representation for the magnetostriction energy in the special case that

$$\Omega = G := \left(-\frac{1}{2}, \frac{1}{2}\right)^2.$$

For the remainder of the paper, it is this cross-section that we will work with.

Lemma 2.3. *Let $V \in L^2(G; \mathbb{R}^{2 \times 2})$. Then*

$$\inf_{\mathbf{u} \in H^1(G; \mathbb{R}^2)} \int_G \|\epsilon(\mathbf{u}) - V\|^2 d\mathbf{x} = \sum_{\mathbf{k} \in \mathbb{Z}^2 \setminus \{0\}} \frac{1}{|\mathbf{k}|^4} \left(|\mathbf{k}|^4 \|\widehat{V}(\mathbf{k})\|^2 - 2|\mathbf{k}|^2 |\widehat{V}(\mathbf{k})\mathbf{k}|^2 + |\mathbf{k} \cdot \widehat{V}(\mathbf{k})\mathbf{k}|^2 \right), \quad (2.8)$$

with

$$\widehat{V}(\mathbf{k}) := \int_G V(\mathbf{x}) e^{-2\pi i \mathbf{k} \cdot \mathbf{x}} d\mathbf{x}.$$

Proof. Let V be as in the Lemma, and let u_0 denote the minimizer obtained from Theorem 2.2. We know that $u_0 \in H^1(G)$ are weak solutions of the Euler-Lagrange equations given by

$$\begin{aligned} \operatorname{div}(\epsilon(u_0) - V) &= 0, & \mathbf{x} &\in G, \\ (\epsilon(u_0) - V) \nu &= 0, & \mathbf{x} &\in \partial G \setminus C \end{aligned}$$

with C denoting the corners of the domain G . Consider now the larger square $G^* := (-\frac{1}{2}, \frac{3}{2}) \times (-\frac{1}{2}, \frac{3}{2})$; see Figure 2 below.

We define V^* on G^* as follows: first, define $V^* = V$ on $G \subset G^*$. On the square $(\frac{1}{2}, \frac{3}{2}) \times (-\frac{1}{2}, \frac{1}{2})$ we define V^* by performing an even reflection of V in the x -variable about the side $\{x = \frac{1}{2}\} \cap \overline{G}$. Finally, we define V^* on the rectangle $(-\frac{1}{2}, \frac{3}{2}) \times (\frac{1}{2}, \frac{3}{2})$ by an even reflection in the y -variable of V^* defined thus far, about the line $\{y = \frac{1}{2}\} \cap G^*$. We denote by u_0^* the result of performing the foregoing reflection procedure to u_0 . It is clear, thanks to the even reflection that $u_0^* \in H^1(G^*)$, and is G^* -periodic. We now consider the variational problem

$$\inf_{w \in H_{\#}^1(G^*; \mathbb{R}^2)} \int_{G^*} \|\epsilon(w) - V^*\|^2 d\mathbf{x}, \quad (2.9)$$

where $H_{\#}^1(G^*; \mathbb{R}^2)$ consists of G^* -periodic H^1 vector fields in \mathbb{R}^2 . We note that up to addition of constants and infinitesimal rotations, this problem has a unique minimizer. We claim that $u_0^* \in H_{\#}^1(G^*)$ is a minimizer to this variational problem. Indeed, by convexity,

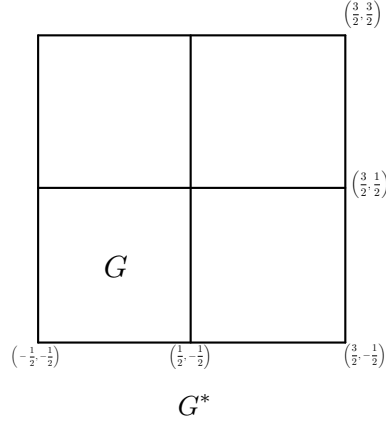


Figure 2: The construction in the proof of Lemma 2.3

it suffices to verify the weak form of the Euler-Lagrange equations. In fact, it suffices to verify the weak form of the Euler-Lagrange equations associated to (2.9) in neighborhoods of points along ∂G^* (away from the corners). To this end, we let $B = B(\mathbf{x}, r)$ denote a ball centered at $\mathbf{x} \in \partial G^* \setminus C$ and radius $r < 1$. We test against functions $\phi \in C_c^\infty(B; \mathbb{R}^2)$, and we write $B = B_+ \cup B_-$ with $B_+ = B \cap G^*$ and $B_- = B \setminus \overline{G^*}$. By integration by parts, we find

$$\begin{aligned} \int_B \epsilon(\phi) : (\epsilon(u_0^*) - V^*) \, d\mathbf{x} &= - \int_{B_+} \phi \cdot \operatorname{div} (\epsilon(u_0^*) - V^*) \, d\mathbf{x} - \int_{B_-} \phi \cdot \operatorname{div} (\epsilon(u_0^*) - V^*) \, d\mathbf{x} \\ &\quad + \int_{\partial G \cap B} \phi \cdot (\epsilon(u_0^*) - V^*)_+ \nu - \int_{\partial G \cap B} \phi \cdot (\epsilon(u_0^*) - V^*)_- \nu \\ &= 0, \end{aligned}$$

thanks to the Euler-Lagrange equations satisfied by u_0 , and crucially, the natural boundary conditions. Here, subscripts \cdot_\pm respectively denote the traces of the periodized quantities along ∂G^* .

Having shown this, the Fourier representation follows as in the proof of [13, Lemma 4.1]. \square

Remark 2.4. We point out that one can think of the foregoing theorem as a consequence of the Paley-Wiener and Plancherel-Polya inequality discussion from Section 2.1, applied to the compactly supported distributions u_0 and V on \mathbb{R}^2 by extending these trivially outside G .

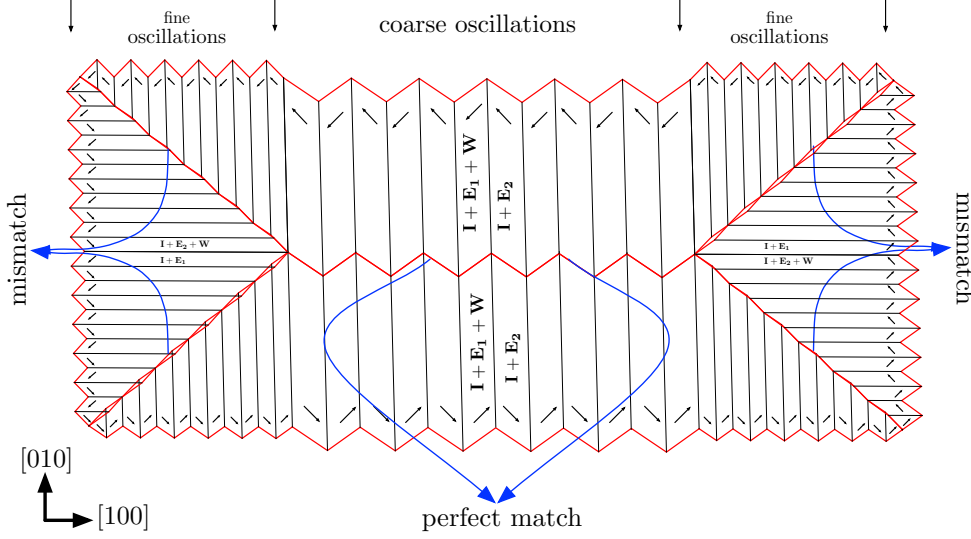


Figure 3: Deformed zig-zag Landau state with no transition layer. The preferred strains: \mathbf{E}_1 and \mathbf{E}_2 and the infinitesimal rotation \mathbf{W} are given in equation (56) of [5] .

3 Upper bound: the results of [5] and a modification

In our previous paper [5], the energies of laminates of the normal Landau state and of the zig-zag Landau state were compared. The zig-zag Landau state refers to the magnetization pattern reported in the experiments of Chopra and Wuttig [4], also see Figure 1(b) and 1(c), whereas, the normal Landau state is the magnetization pattern observed in more traditional cubic materials such as Permalloy, see Figure 1(a).

At the level of energies, comparing the two in the parameter regimes of Galfenol shows that the zig-zag Landau state is energetically favored compared to the normal Landau state. This is striking, because the zig-zag Landau state is a significantly more complex, two scale construction, as opposed to a single-scale normal Landau state laminate. We showed in [5] that the zig-zag Landau state has a coarse microstructure in regions of mechanical compatibility of the preferred strain and a fine scale microstructure near the regions of incompatibility of the preferred strain, refer to the discussion in [5, Section 2.1 and Lemma 4.2].

Towards recalling this construction and presenting a different version of it, we note that the easy axes of a cubic material consists of $\left\{ \left(\pm \frac{1}{\sqrt{2}}, \pm \frac{1}{\sqrt{2}} \right) \right\}$, and thus, two kinds of walls

make up most of our constructions: 90° walls, and 180° walls. In [5], we made a construction which was divergence free, motivated by the large K_d -value for Galfenol. Here, we briefly present a slight modification of that construction that is relevant for cubic ferromagnets with large and comparable magnetostriction and magnetostatic energies and significantly larger magnetocrystalline anisotropy.

The fundamental building block of both constructions is the single zig-zag Landau state unit cell, shown in Figure 3. Both our constructions consist in the bulk of $k \in \mathbb{N}$ single zig-zag Landau states in the sample G . It is easily checked that the number of 180° walls is comparable to k . In regions of mechanical incompatibility, the zig-zag Landau state construction consists of a further fine-scale oscillation that predominantly makes use of ‘ l ’ 90° – walls.

The difference between the constructions we presented in [5] and the modification we describe here lies in the triangular boundary domains. In the construction in [5], these consisted of closure domains where the magnetization *does not* lie along the easy axes, but is divergence free. In the modification we present in Figure 4, the magnetization is *not* divergence-free, but lies on the easy axes. We have highlighted the magnetization in four representative boundary triangles in Figure 4.

This magnetization pattern \mathbf{m} is shown in Figure 4, where $k = 2$. In this construction $\mathbf{m} \in \{\pm \mathbf{m}_1, \pm \mathbf{m}_2\}$, and so this construction has zero anisotropy energy.

Aside from the boundary triangles described above, the modification in 4 is identical to the constructions in [5]: each zig-zag Landau state is a second order laminate consisting of two distinct scales of oscillation frequencies, a coarse scale oscillation of frequency $k \sim \frac{L^{\frac{1}{3}}(c_{44}\lambda_{111}^2 + K_d)^{\frac{1}{3}}}{\gamma^{\frac{1}{3}}}$ and a fine scale oscillation of frequency $lk \sim \frac{L^{\frac{2}{3}}(c_{44}\lambda_{111}^2 + K_d)^{\frac{2}{3}}}{\gamma^{\frac{2}{3}}}$.

Calculating the energies of the both constructions is identical with the exception that the present construction also has a magnetostatic contribution. We remind the reader that in [5] we worked with the sharp interface energy, which prior to non-dimensionalizing reads

$$\mathbb{R}_\#(\mathbf{m}) = \mu L \int_G |\nabla \mathbf{m}| + K_a L^2 \int_G \varphi(\mathbf{m}) d\mathbf{x} + K_d L^2 \int_{\mathbb{R}^2} |\mathbf{h}_\mathbf{m}|^2 d\mathbf{x} + c_{44} \lambda_{111}^2 e_{mag}(\mathbf{m}), \quad (3.1)$$

with competitors that satisfied $\mathbf{m} \in BV(G; \mathbb{R}^2)$. Estimating the magnetostriction energy of this magnetization proceeds identically to [5]: for a detailed description of the magnetization, and the deformation gradients in the sample G away from the boundary triangles which remain unchanged for the present construction, we refer the reader to [5, Section 4.3].

It remains to estimate the magnetostatic energy of our construction in Figure 4. We make use of

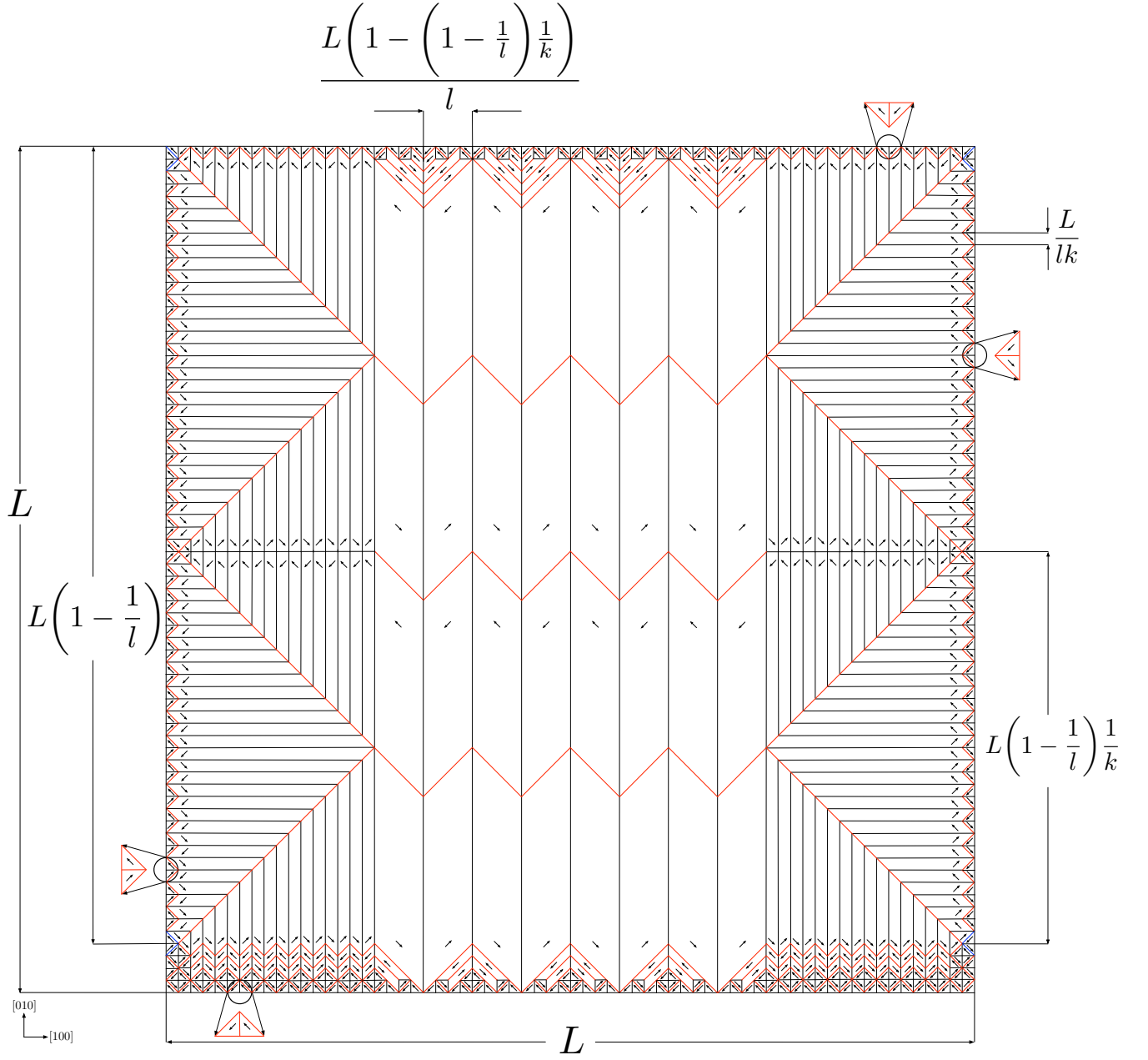


Figure 4: Magnetization in $(-\frac{L}{2}, \frac{L}{2}) \times (-\frac{L}{2}, \frac{L}{2})$ square consisting of k zig-zag Landau states for cubic ferromagnet with large and comparable magnetostriction and magnetostatic energies. Note that the magnetization in the boundary triangles is not divergence free.

Lemma 3.1. *Let $\mathbf{m} \in L^2(G; \mathbb{R}^2)$ be a magnetization pattern, and let $\mathbf{h}_\mathbf{m} \in L^2(\mathbb{R}^2, \mathbb{R}^2)$ denote the corresponding induced magnetic field that satisfies Maxwell's equations of magnetostatics (1.23a, 1.23b) in the sense of distributions. Then*

$$\int_{\mathbb{R}^2} |\mathbf{h}_\mathbf{m}|^2 d\mathbf{x} \leq \int_G |\mathbf{m}|^2 d\mathbf{x}.$$

In fact,

$$\int_{\mathbb{R}^2} |\mathbf{h}_\mathbf{m}|^2 d\mathbf{x} = \min_{\mathbf{n} \in \mathcal{B}} \int_{\mathbb{R}^2} |\mathbf{n}|^2 d\mathbf{x},$$

with

$$\mathcal{B} := \{\mathbf{n} \in L^2(\mathbb{R}^2; \mathbb{R}^2) : \int_{\mathbb{R}^2} (\mathbf{n} + \mathbf{m}) \cdot \nabla \psi d\mathbf{x} = 0 \text{ for every } \psi \in H^1(\mathbb{R}^2)\}.$$

Proof. Let $\mathbf{h}_\mathbf{m} = -\nabla \chi$ where $\chi \in H^1(\mathbb{R}^2, \mathbb{R}^2)$. The short proof of this lemma is, for any $\mathbf{n} \in \mathcal{B}$, we have

$$\begin{aligned} \int_{\mathbb{R}^2} |\mathbf{n}|^2 d\mathbf{x} &= \int_{\mathbb{R}^2} |\mathbf{n} - \mathbf{h}_\mathbf{m}|^2 + |\mathbf{h}_\mathbf{m}|^2 + 2\langle (\mathbf{n} - \mathbf{h}_\mathbf{m}), \mathbf{h}_\mathbf{m} \rangle d\mathbf{x} \\ &\geq \int_{\mathbb{R}^2} |\mathbf{h}_\mathbf{m}|^2 - 2 \int_{\mathbb{R}^2} \langle \mathbf{n} + \mathbf{m}, \nabla \chi \rangle \\ &= \int_{\mathbb{R}^2} |\mathbf{h}_\mathbf{m}|^2 d\mathbf{x}, \end{aligned}$$

where in the second-to-last line, we have used Maxwell's equations and the fact that $\mathbf{n} \in \mathcal{B}$. We note that we have equality if and only if $\mathbf{n} = \mathbf{h}_\mathbf{m}$. \square

Observe that the above lemma does *not* require that the test vector field \mathbf{n} has support equal to that of \mathbf{m} ; in fact, the vector field \mathbf{n} is not even required to be S^1 -valued in the domain. We choose the test function \mathbf{n} as follows: $\mathbf{n} = -\mathbf{m}$ on the boundary triangles and zero elsewhere, so that \mathbf{n} is supported on the boundary triangles. Since $\operatorname{div} \mathbf{n} = -\operatorname{div} \mathbf{m}$ in the sense of distributions on \mathbb{R}^2 , by Lemma 3.1, we have

$$K_d \int_{\mathbb{R}^2} |\mathbf{h}_\mathbf{m}|^2 d\mathbf{x} \leq K_d \int_{\mathbb{R}^2} |\mathbf{n}|^2 d\mathbf{x} = K_d \int_{\text{bdry. triangles}} |\mathbf{n}|^2 d\mathbf{x} \sim K_d \times \frac{L^2}{lk}$$

Hence, arguing as in [5], the total sharp interface micromagnetic energy $\mathbb{F}_\#(\mathbf{m})$ has three contributions, estimated by

$$\mathbb{F}_\#(\mathbf{m}) \lesssim \underbrace{\gamma Lk}_{180^\circ \text{ degree wall energy}} + \underbrace{\gamma Ll}_{90^\circ \text{ degree wall energy}} + \underbrace{\left\{ c_{44} \lambda_{111}^2 + K_d \right\} \times \frac{L^2}{lk}}_{\text{magnetostriction and magnetostatic energy}}. \quad (3.2)$$

Optimizing equation (3.2) with respect to l and k we obtain our upper bound for a cubic ferromagnet with large and comparable magnetostriction and magnetostatic energies, both of which are dominated by the anisotropy energy. Returning to our non-dimensional units and by standard facts about the Modica-Mortola $\eta \rightarrow 0$ asymptotics, the upper bound stated in Theorem 1.1 follows.

3.1 Branching constructions

The goal of this section is to compare the zig-zag Landau state construction with other constructions observed in micromagnetics, primarily the normal Landau state laminate as seen in Permalloy, and constructions based on branching, studied in detail in [2].

First, in Permalloy, it is easy to understand why one sees the normal Landau-state laminate: here, the value of the magnetostriction contribution $c_{44}\lambda_{111}^2$ is extremely small, as compared to the anisotropy and demagnetization, refer to [5] for details. As argued in [5], in this parameter regime, the normal Landau state has lower energy scaling than the zig-zag Landau state.

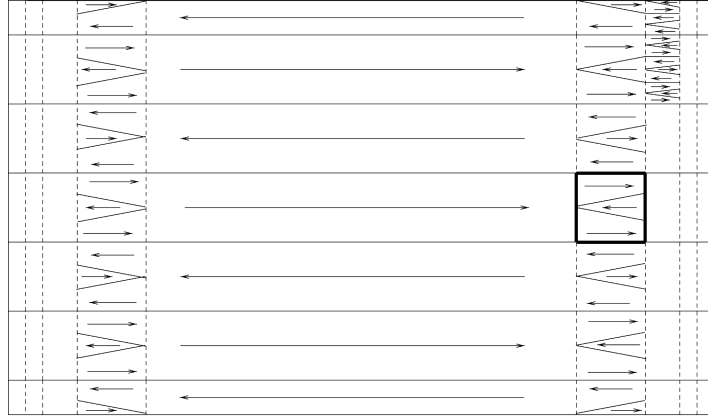
Material parameters	Galfenol	Permalloy	Iron
A	10^{-12} J/m	10^{-12} J/m	10^{-12} J/m
K_a	$-3 \times 10^3 \text{ J/m}^3$	$-1.7 \times 10^2 \text{ J/m}^3$	$4.8 \times 10^4 \text{ J/m}^3$
K_d	$1.06 \times 10^6 \text{ J/m}^3$	$5 \times 10^5 \text{ J/m}^3$	10^6 J/m^3
$c_{44}\lambda_{111}^2$	$1.06 \times 10^3 \text{ J/m}^3$	10^{-1} J/m^3	10^2 J/m^3

Table 1: Material parameters of Galfenol, Permalloy and Iron. Exchange stiffness: A , anisotropy energy coefficient: K_a , magnetostatic energy coefficient: $K_d = J_s^2/2\mu_0$ and magnetostriction energy coefficient: $c_{44}\lambda_{111}^2$.

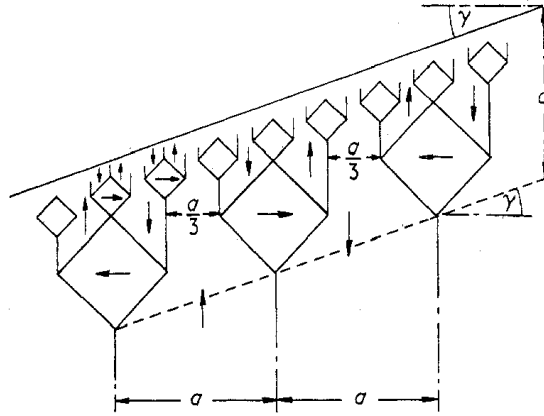
Next we turn our attention to magnetic microstructures in Iron, cf. Figure 5. In the rest of this section, we argue that, interestingly, the energy scaling of “branched” constructions that one sees in these settings is identical to that of the zig-zag Landau state. Branched magnetic microstructures are analytically captured via the Privorotskii construction, which we next briefly digress recall following [2].

On Privorotskii constructions in light of magnetostriction:

The authors in [2] detail two “Privorotskii” constructions, one that is divergence-free [2, Figure 2.2], and one that is anisotropy-free [2, Figure 3.1]. While the magnetostriction energy contribution is not included in the uniaxial context considered in [2], it is easy to estimate the contribution of this energy for these constructions. For the anisotropy-free



(a)



(b)

Figure 5: (a) Branching in uniaxial materials: anisotropy-free Privorotskii's construction, see [3]. (b) Branching in cubic materials: Privorotskii's construction for cubic materials, see [17]

construction, the magnetostriction energy is zero, because this construction only makes use of one pair of easy axes, say $\pm \mathbf{m}_1$. Since the preferred strain tensor $\epsilon_0(\mathbf{m})$ is an even function of \mathbf{m} , it follows that the corresponding minimizing strain for the magnetostriction energy is equal to the preferred strain, hence resulting in zero magnetostriction energy. Consequently, working with the dimensional micromagnetic energy, the scaling law for this construction is given by $A^{2/3}(K_d L^2)^{1/3}$.

Turning to the magnetostriction energy of the divergence-free Privorotskii construction, the estimate of the magnetostriction contribution is just as easy: as a competitor, setting $\epsilon(\mathbf{u}) = \epsilon_0(\mathbf{m}_1)$, the magnetostriction contribution only arises from regions where the magnetocrystalline anisotropy is penalized. In other words, the scaling of this construction including magnetostriction is $A^{2/3}(K_d + c_{44}\lambda_{111}^2)^{1/3}L^{2/3}$.

In the context of Iron, Lifshitz conjectured, [14, Figure 2], and Privorotskii constructed an upper bound for cubic ferromagnets which displayed branching, refer to Figure 5. A calculation as in [2] shows that the energy for this construction also scales as $A^{2/3}(K_d + c_{44}\lambda_{111}^2)^{1/3}L^{2/3}$. For concreteness, let us compare two specific ansatzes: the zig-zag Landau state, studied in this paper and in [5], and variations of Privorotskii's constructions, studied in [2]; see also [17] for a construction in the case of cubic ferromagnets. The foregoing discussions indicate that at the level of energy scaling, both sets of constructions achieve the 2/3-scaling, and are hence optimal in scaling, in accordance with the lower bound proof in this paper. However, arguing as in [5], one can show that the average strains corresponding to the various Privorotskii constructions *do not* match with those from experiments on Galfenol, [4]. It was in fact for this reason that in [5], we pursued a detailed construction of the zig-zag Landau state, and computed that the average strains for this construction corresponds to those obtained from experiments. The situation is, however, different for Iron, which predominantly demonstrates branching as in the Privorotskii construction, refer to [14, 11, 17]. Looking at Table 3.1, it is clear that the magnetostriction constant in Iron are significantly higher than those in Permalloy, while those in Galfenol are higher still. The authors in [3] raised the question of understanding branching in Iron in the context of scaling laws of micromagnetic energy plus magnetostriction. While our paper presents a contribution towards answering this question in a two-dimensional setting, it naturally raises the following question: beyond optimal energy scaling laws, what are other selection criteria in pattern selection within cubic ferromagnets, that also correctly predict the observed macroscopic strain from experiments?

4 Proof of the lower bound

The goal of this section is to prove Theorem 1.1

Proof of Theorem 1.1. The proof of the upper bound follows easily from the discussion in Section 3, and expressing the construction there in the non-dimensional units. It remains to prove the lower bound. The proof of the lower bound theorem proceeds in several steps.

Step 0. For any $\eta > 0$, let $v_\eta \in H^1(G; \mathbb{R}^2)$ denote a minimizer of the energy \mathcal{F}_η . The existence of such a minimizer follows by an easy application of the direct method in the Calculus of variations. By the upper bound construction, $F_\eta(v_\eta) \lesssim \mu^{2/3}$. By the De Simone-Kohn-Müller-Otto compactness theorem [9], after passing to a sub-sequence that is not denoted, $v_\eta \rightarrow \mathbf{m}$ strongly in $L^2(G; \mathbb{R}^2)$ where $|\mathbf{m}| = 1$ almost everywhere in G . Furthermore, thanks to the bound on the magnetocrystalline anisotropy, we in fact have $\mathbf{m} \in \left\{ \left(\pm \frac{1}{\sqrt{2}}, \pm \frac{1}{\sqrt{2}} \right) \right\}$ almost everywhere in G .

Let \mathbf{u}_η denote the displacement associated to v_η , guaranteed by Theorem 2.2. It follows then that $\mathbf{u}_\eta \rightarrow \mathbf{u}$ strongly in $H^1(G; \mathbb{R}^2)$ where \mathbf{u} is the displacement associated to \mathbf{m} ; furthermore, we have

$$\int_G \|\epsilon(\mathbf{u}) - \epsilon_0(\mathbf{m})\|^2 d\mathbf{x} = \lim_{\eta \rightarrow 0} \|\epsilon(\mathbf{u}_\eta) - \epsilon_0(v_\eta)\|^2 d\mathbf{x}. \quad (4.1)$$

Finally, by the Modica-Mortola inequality [19], and using the fact that $\mathbf{m} \in \left\{ \left(\pm \frac{1}{\sqrt{2}}, \pm \frac{1}{\sqrt{2}} \right) \right\}$ almost everywhere in G , we find that

$$\mu \int_G |\nabla \mathbf{m}| \lesssim \liminf_{\eta \rightarrow 0} \int_G \mu \eta |\nabla v_\eta|^2 + \frac{\mu}{\eta} \varphi(v_\eta) \leq \liminf_{\eta \rightarrow 0} F_\eta(v_\eta). \quad (4.2)$$

For the convenience of the reader, we summarize the structure of the proof:

- In Step 1, we simplify the magnetostriction energy in Fourier space. The key idea is to write this energy in terms of a Fourier multiplier acting on the oscillatory function $m_1 m_2$ which is $\pm \frac{1}{2}$ -valued on G . Note that the quantity $m_1 m_2$ corresponds to the off-diagonal terms in the preferred strain matrix $\epsilon_0(\mathbf{m})$, and changes sign on G , while the diagonal terms of $\epsilon_0(\mathbf{m})$ are constant and equal to $\frac{1}{2}$.
- In Step 2, we decompose the minimizing magnetization \mathbf{m} in Fourier space, via a sort of laminate decomposition. This step follows the arguments in [13].
- In Step 3, we obtain a lower bound on the sum of the exchange and magnetostriction energies, along with an interpolation inequality from [3]. This permits us to complete the lower bound in the case when the magnetization is, roughly speaking, equally distributed among the four easy axes, so that $\int_G m_1 m_2 d\mathbf{x} \sim 0$. It is in this context that the magnetostriction contribution is large.

- In the last step, Step 4, we deal with the case when the magnetization lies predominantly in one pair of easy axes, either $\pm(\frac{1}{\sqrt{2}}, \frac{1}{\sqrt{2}})$ or $\pm(-\frac{1}{\sqrt{2}}, \frac{1}{\sqrt{2}})$, or equivalently, $\int_G m_1 m_2 d\mathbf{x}$ is big. In this case, the magnetization is predominantly uniaxial, and the required lower bound follows from [3].

Step 1. The goal of this step is to simplify the magnetostriction energy. Let \mathbf{m} be as in Step 0. We note that $V = \epsilon_0(\mathbf{m})$ is in $L^p(G; \mathbb{R}^{2 \times 2})$ and is compactly supported for each $p \in [1, \infty]$. Let $\mathbf{u} \in H^1(G; \mathbb{R}^2)$ with $\int_\Omega \mathbf{u} d\mathbf{x} = 0$, and note that this mean-zero condition is merely a choice: in the following estimates it is convenient to arrange

$$\frac{\langle \nabla \mathbf{u} \rangle + \langle \nabla \mathbf{u} \rangle^T}{2} = \langle V \rangle. \quad (4.3)$$

We continue to denote the resulting translated \mathbf{u} by \mathbf{u} . Identifying the L^2 function $\frac{\nabla \mathbf{u} + \nabla \mathbf{u}^T}{2}$ with its extension by 0 outside G , we fall in the setting of the Schwartz's Paley-Wiener Theorem discussed Section 2.1. Taking into account Lemma (2.3)-Equation (2.8), (2.5), and (4.3),

$$\int_G \|\epsilon(\mathbf{u}) - V\|^2 d\mathbf{x} = \sum_{\mathbf{k} \in \mathbb{Z}^2, \mathbf{k} \neq 0} \frac{1}{|\mathbf{k}|^4} \left| |\mathbf{k}|^4 \|\widehat{V}(\mathbf{k})\|^2 - 2|\mathbf{k}|^2 |\widehat{V}(\mathbf{k})\mathbf{k}|^2 + |\mathbf{k} \cdot \widehat{V}(\mathbf{k})\mathbf{k}|^2 \right|^2, \quad (4.4)$$

with $\widehat{V}(\mathbf{k})$ being defined by (2.3). Since $m_1^2 = m_2^2 = \frac{1}{2}$ in G , it follows that for $\mathbf{k} \in \mathbb{Z}^2 \setminus \{0\}$, the extension of these functions by zero outside G satisfies $\widehat{m}_1^2(\mathbf{k}) = \widehat{m}_2^2(\mathbf{k}) = 0$. Towards using (4.4), for $\mathbf{k} \neq 0$, the matrix $\widehat{V}(\mathbf{k})$ takes the form

$$\widehat{V}(\mathbf{k}) = \frac{3}{2} \begin{pmatrix} 0 & b_k \\ b_k & 0 \end{pmatrix} \quad (4.5)$$

with

$$b_k = \widehat{m_1 m_2}(\mathbf{k}). \quad (4.6)$$

It is this structure of the matrices $\widehat{V}(\mathbf{k})$ significantly simplifies (4.4) and lies at the heart of our paper. Indeed, plugging in (4.5) into (4.4), we find that for each \mathbf{k} , since

$$|\mathbf{k}|^4 \|\widehat{V}(\mathbf{k})\|^2 - 2|\mathbf{k}|^2 |\widehat{V}(\mathbf{k})\mathbf{k}|^2 = 0,$$

one has

$$\int_G \|\epsilon(\mathbf{u}) - \epsilon_0(\mathbf{m})\|^2 d\mathbf{x} = \sum_{\mathbf{k} \in \mathbb{Z}^2, \mathbf{k} \neq 0} \frac{1}{|\mathbf{k}|^4} |2b_k k_1 k_2|^2 \quad (4.7)$$

Step 2: In this step, we decompose the magnetization \mathbf{m} in Fourier space. To this end, let S^1 denote the unit circle in Fourier space: $S^1 := \{\hat{k} \in \mathbb{R}^2 : \hat{k}_1^2 + \hat{k}_2^2 = 1\}$. Consider the open cover $\{U_j\}_{j=1}^2$ of S^1 defined by

$$U_1 := \{\hat{k} \in S^1 : \hat{k}_2^2 < \hat{k}_1^2\}, \quad U_2 := \{\hat{k} \in S^1 : \hat{k}_2^2 > \frac{3}{4}\hat{k}_1^2\}.$$

For use in the next step, we record that the trivial estimates that for any $k \in \mathbb{R}^2 \setminus \{0\}$ whose projection onto S^1 lies on U_1 , one has

$$\frac{k_1^2 k_2^2}{(k_1^2 + k_2^2)^2} > \frac{1}{2} \frac{k_2^2}{k_1^2 + k_2^2}, \quad (4.8)$$

while for any $k \in \mathbb{R}^2 \setminus \{0\}$ whose projection lies on U_2 one has the inequality

$$\frac{k_1^2 k_2^2}{(k_1^2 + k_2^2)^2} > \frac{3}{7} \frac{k_1^2}{k_1^2 + k_2^2}. \quad (4.9)$$

Let now $\{\tilde{\eta}_j\}_{j=1}^2$ be a smooth partition of unity subordinate to the cover $\{U_j\}_{j=1}^2$, satisfying $\tilde{\eta}_j$ are nonnegative, even, supported respectively on U_j , and $\sum_{j=1}^2 \tilde{\eta}_j(\hat{k}_1, \hat{k}_2) \equiv 1$ on S^1 . With an eye towards defining Fourier multipliers that are smooth away from the origin and verify the conditions of the Hörmander-Mikhlin multiplier theorem, define $\eta_j : \mathbb{R}^2 \rightarrow [0, \infty)$ by $\eta_j(k) := \tilde{\eta}_j\left(\frac{k}{|k|}\right)$ for $k \neq 0$ and $\eta_j(0) = 0$. For any $h \in L^p(\mathbb{R}^2)$, $p \in (1, \infty)$, defining the operator T_j in Fourier space by

$$\widehat{T_j h}(\xi) = \sqrt{\eta_j(\xi)} \widehat{h}(\xi), \quad (4.10)$$

the Hörmander-Mikhlin multiplier theorem, [18, Theorem 3.8 and Corollary 3.16] entail that $T_j : L^p(\mathbb{R}^2) \rightarrow L^p(\mathbb{R}^2)$ is a bounded linear operator. We will make use of this operator below to define a certain decomposition of the magnetization into “laminates”.

Recall from Step 1 that

$$\int_G \|\epsilon(\mathbf{u}) - \epsilon_0(\mathbf{m})\|^2 d\mathbf{x} = \sum_{\mathbf{k} \in \mathbb{Z}^2 \setminus \{0\}} \frac{4k_1^2 k_2^2}{(k_1^2 + k_2^2)^2} |b_k|^2. \quad (4.11)$$

Before proceeding, we define a decomposition of the magnetization profile into a pair of “laminates”, one of which is predominantly along the x -direction and the other which is predominantly along the y -direction. More precisely, we define, for $\mathbf{k} \in \mathbb{Z}^2 \setminus 0$, and $j = 1, 2$

$$\hat{f}_j(\mathbf{k}) := T_j(\widehat{m_1 m_2})(\mathbf{k}) = \sqrt{\eta_j(\mathbf{k})} \widehat{m_1 m_2}(\mathbf{k}) = \sqrt{\eta_j(\hat{k})} b_k, \quad (4.12)$$

using the operator T_j from (4.10). Continuing from (4.11), inserting the definitions (4.12), and subsequently the lower bounds (4.8)-(4.9), we find

$$\begin{aligned}
\int_G \|\epsilon(\mathbf{u}) - \epsilon_0(\mathbf{m})\|^2 d\mathbf{x} &= \sum_{\mathbf{k} \in \mathbb{Z}^2 \setminus \{0\}} \frac{4k_1^2 k_2^2}{(k_1^2 + k_2^2)^2} (\eta_1(\hat{k}) + \eta_2(\hat{k})) |b_k|^2 \\
&= \sum_{\mathbf{k} \in \mathbb{Z}^2 \setminus \{0\}} \frac{4k_1^2 k_2^2}{(k_1^2 + k_2^2)^2} (|\hat{f}_1(\mathbf{k})|^2 + |\hat{f}_2(\mathbf{k})|^2) \\
&\gtrsim \sum_{\mathbf{k} \in \mathbb{Z}^2 \setminus \{0\}} \frac{1}{k_1^2 + k_2^2} (k_2^2 |\hat{f}_1(\mathbf{k})|^2 + k_1^2 |\hat{f}_2(\mathbf{k})|^2) \\
&\gtrsim (\|f_1\|_{H^{-1}(\mathbb{R}^2)}^2 + \|f_2\|_{H^{-1}(\mathbb{R}^2)}^2), \tag{4.13}
\end{aligned}$$

where in the last line, we have once again used the Plancherel-Polya inequality and its consequences.

Step 3: In this step, we obtain the desired lower bound on the sum of the exchange energy and the results of Step 3, viz. the sum of anisotropic and magnetostriction energies. The proof involves the application of an interpolation inequality, [3], which is by now well-used in studies on energy-driven pattern formation. To this end, we first obtain a lower bound on the exchange energy in terms of the f_j 's. We begin with the observation that for each $j = 1, 2$, we have that for $\mathbf{k} \neq 0$,

$$|\hat{f}_j(\mathbf{k})|^2 \leq |\widehat{m_1 m_2}(\mathbf{k})|^2$$

Consequently, it follows that for any vector $\mathbf{h} \in \mathbb{R}^2$ we have

$$\sum_{\mathbf{k} \in \mathbb{Z}^2} 4 \sin^2(\pi \mathbf{k} \cdot \mathbf{h}) |\hat{f}_j(\mathbf{k})|^2 \leq \sum_{\mathbf{k} \in \mathbb{Z}^2} 4 \sin^2(\pi \mathbf{k} \cdot \mathbf{h}) |\widehat{m_1 m_2}(\mathbf{k})|^2$$

Using the notation $\Delta_{\mathbf{h}} f(\cdot) := f(\cdot + \mathbf{h}) - f(\cdot)$, we have in physical space,

$$\int_G |\Delta_{\mathbf{h}} m_1|^2 d\mathbf{x} + \int_G |\Delta_{\mathbf{h}} m_2|^2 d\mathbf{x} \gtrsim \int_G |\Delta_{\mathbf{h}}(m_1 m_2)|^2 d\mathbf{x}. \tag{4.14}$$

Identifying $\Delta_{\mathbf{h}}(m_1 m_2)$ with its extension by zero outside G as an $L^2(\mathbb{R}^2)$ function, and repeating earlier arguments using (2.5), we find

$$\begin{aligned}
\int_{\mathbb{R}^2} |\Delta_{\mathbf{h}}(m_1 m_2)|^2 d\mathbf{x} &= \sum_{\mathbf{k} \in \mathbb{Z}^2} 4 \sin^2(\pi \mathbf{k} \cdot \mathbf{h}) |b_k|^2 \gtrsim \sum_{\mathbf{k} \in \mathbb{Z}^2} 4 \sin^2(\pi \mathbf{k} \cdot \mathbf{h}) \sum_{j=1}^2 |\hat{f}_j(\mathbf{k})|^2 \\
&= \sum_{\mathbf{k} \in \mathbb{Z}^2} \sum_{j=1}^2 |\widehat{\Delta_{\mathbf{h}} f_j}(\mathbf{k})|^2 = \sum_{j=1}^2 \int_{\mathbb{R}^2} |\Delta_{\mathbf{h}} f_j|^2 d\mathbf{x}. \tag{4.15}
\end{aligned}$$

Before proceeding, we record an easy estimate concerning the finite difference operator $\Delta_{\mathbf{h}}$. Thanks to the fundamental theorem of Calculus, we have for any $g \in W^{1,1}(G)$ that

$$\|\Delta_{\mathbf{h}}g\|_{L^1}^2 \lesssim |\mathbf{h}| \|g\|_{L^\infty} \int_G |\nabla g| d\mathbf{x}. \quad (4.16)$$

By density arguments, this estimate also holds for $g \in BV$. Applying this last inequality to $g = m_1 m_2$, and then continuing from (4.15), we find for any $\mathbf{h} \neq 0$ that

$$\int_G |\nabla \mathbf{m}| \geq \frac{1}{|\mathbf{h}|} \int_{\mathbb{R}^2} |\Delta_{\mathbf{h}}(m_1 m_2)|^2 d\mathbf{x} \gtrsim \frac{1}{|\mathbf{h}|} \int_{\mathbb{R}^2} |\Delta_{\mathbf{h}} f_1|^2 + |\Delta_{\mathbf{h}} f_2|^2. \quad (4.17)$$

Taking the supremum over $\mathbf{h} \in \mathbb{R}^2$ with $0 < |\mathbf{h}| < 1$, we recall that a particular Besov seminorm of a function f is equivalently characterized by

$$\|f\|_{\dot{B}_{2,\infty}^{1/2}}^2 := \sup_{0 < |\mathbf{h}| < 1} \frac{1}{|\mathbf{h}|} \int_{\mathbb{R}^2} |\Delta_{\mathbf{h}} f(x)|^2 dx.$$

For later use, we also note that the corresponding full Besov norm is then given by

$$\|f\|_{B_{2,\infty}^{1/2}} := \|f\|_{L^2} + \|f\|_{\dot{B}_{2,\infty}^{1/2}}.$$

With these definitions, we get the bound

$$\|f_1\|_{\dot{B}_{2,\infty}^{1/2}}^2 + \|f_2\|_{\dot{B}_{2,\infty}^{1/2}}^2 \leq \int_G |\nabla \mathbf{m}|. \quad (4.18)$$

Conclusion of Step 3: It remains to combine the results of Steps 2 and 3 so far, by using an interpolation inequality [3]. We have from (4.13) and (4.18), Step 0, Young's inequality, and the interpolation inequality [3, Lemma 2.3 and Remark 3.1] that

$$\begin{aligned} \liminf_{\eta \rightarrow 0} \mathcal{F}_\eta(v_\eta) &\geq \mu \int_G |\nabla \mathbf{m}| + \int_G \|\epsilon(\mathbf{u}) - \epsilon_0(\mathbf{m})\|^2 d\mathbf{x} \\ &\geq \mu \left(\|f_1\|_{\dot{B}_{2,\infty}^{1/2}}^2 + \|f_2\|_{\dot{B}_{2,\infty}^{1/2}}^2 \right) + \left(\|f_1\|_{\dot{H}^{-1}(\mathbb{R}^2)}^2 + \|f_2\|_{\dot{H}^{-1}(\mathbb{R}^2)}^2 \right) \\ &= \mu \left(\|f_1\|_{B_{2,\infty}^{1/2}}^2 + \|f_2\|_{B_{2,\infty}^{1/2}}^2 \right) + \left(\|f_1\|_{\dot{H}^{-1}(\mathbb{R}^2)}^2 + \|f_2\|_{\dot{H}^{-1}(\mathbb{R}^2)}^2 \right) - \mu \left(\|f_1\|_{L^2}^2 + \|f_2\|_{L^2}^2 \right) \\ &\geq c_3 3^{1/3} (3/2)^{2/3} \mu^{2/3} \left(\left(\|f_1\|_{B_{2,\infty}^{1/2}}^{2/3} \|f_1\|_{\dot{H}^{-1}}^{1/3} \right)^2 + \left(\|f_2\|_{B_{2,\infty}^{1/2}}^{2/3} \|f_2\|_{\dot{H}^{-1}}^{1/3} \right)^2 \right) - \mu \left(\|f_1\|_{L^2}^2 + \|f_2\|_{L^2}^2 \right) \\ &\geq (c_3 \mu^{2/3} - \mu) \left(\|f_1\|_{L^2}^2 + \|f_2\|_{L^2}^2 \right) \\ &= \frac{c_3 \mu^{2/3}}{2} \sum_{\mathbf{k} \in \mathbb{Z}^2, \mathbf{k} \neq 0} |b_{\mathbf{k}}|^2, \end{aligned} \quad (4.19)$$

provided $\mu < 1$ is suitably small, say $\mu \leq c_1 < 1$ for a universal constant c_1 depending only on c_3 . Here, up to the universal constant $3^{1/3}(3/2)^{2/3}$, the constant $c_3 > 0$ is the one arising from the quoted interpolation inequality. Let $0 < \delta < \frac{1}{2}$ be a number that will be fixed towards the end of the proof. To complete the proof, we first suppose that the magnetization \mathbf{m} satisfies

$$\left(\int_G m_1 m_2 d\mathbf{x} \right)^2 \leq \frac{1}{4} - \delta^2. \quad (4.20)$$

Adding and subtracting $\mu^{2/3} \left(\int_G m_1 m_2 d\mathbf{x} \right)^2$ to the right hand side of (4.20), it follows by Plancherel's theorem that

$$\liminf_{\eta \rightarrow 0} \mathcal{F}_\eta(v_\eta) \geq \mu^{2/3} \int_G (m_1 m_2)^2 d\mathbf{x} - \mu^{2/3} \left(\int_G m_1 m_2 d\mathbf{x} \right)^2.$$

On the one hand, since $m_1^2 = m_2^2 = \frac{1}{2}$, we have

$$\int_G (m_1 m_2)^2 d\mathbf{x} = \frac{1}{4}.$$

On the other hand, using (4.20), we would have

$$\liminf_{\eta \rightarrow 0} \mathcal{F}_\eta(v_\eta) \gtrsim \delta^2 \mu^{2/3}. \quad (4.21)$$

It remains to make an appropriate choice of δ , this will be done at the end of the next step. Our choice will entail that when $\beta \leq c_2$, then $\frac{1}{4} > \delta^2 \geq c_3 \beta^{1/3}$. Thus, making the choice of δ will complete the proof under the assumption (4.20).

Step 4: In this step, we suppose instead of (4.20), we have the inequality

$$\frac{1}{4} - \delta^2 < \left(\int_G m_1 m_2 d\mathbf{x} \right)^2 \leq \frac{1}{4}. \quad (4.22)$$

Magnetizations that satisfy such an inequality are similar to the anisotropy-free Privorotskii construction, where \mathbf{m} only uses one pair of easy axes. Before providing the details of the proof, we sketch some heuristics. Suppose for instance $\int_G m_1 m_2 d\mathbf{x} > 0$ and satisfies the inequality in (4.22). In this case, \mathbf{m} is essentially uniaxial and only takes values in $\pm \left(\frac{1}{\sqrt{2}}, \frac{1}{\sqrt{2}} \right)$. Concerning the magnetostriction energy, the preferred strain $\epsilon_0(\mathbf{m})$ is an even function of \mathbf{m} , and hence, we expect the magnetostriction energy corresponding to such a magnetization to be small. On the other hand, in this essentially uniaxial regime, obtaining a lower bound for the sum of the exchange and magnetostatic energy was exactly the content of [3]: we thus make use of the result of this paper, and we obtain an

error term owing to the fact that \mathbf{m} is only approximately uniaxial. It is this error term which sets the value of δ , making use of the parameter regime relating μ and Q .

We turn now to implementing this program. We assume throughout that $\int_G m_1 m_2 d\mathbf{x} > 0$ and satisfies (4.22). The proof in the case when $\int_G m_1 m_2 d\mathbf{x} < 0$ and satisfies (4.22) is completely analogous. By Cauchy-Schwarz applied to the magnetostatic energy, we find

$$\|\operatorname{div} \mathbf{m}\|_{H^{-1}}^2 = \|m_{1,x} + m_{2,y}\|_{H^{-1}}^2 \geq \frac{1}{2} \|m_{1,x} + m_{1,y}\|_{H^{-1}}^2 - \|m_{1,y} - m_{2,y}\|_{H^{-1}}^2.$$

Thanks to $\int_G m_1 m_2 d\mathbf{x} > 0$ and (4.22), we find $\int_G (m_1 - m_2)^2 d\mathbf{x} \leq \delta^2$. This in turn implies that

$$\|m_{1,y} - m_{2,y}\|_{H^{-1}} = \sup_{\zeta \in H_0^1, \|\nabla \zeta\|_{L^2} \leq 1} \int_G (m_1 - m_2) \partial_y \zeta dx dy \leq \delta.$$

It follows then that

$$\liminf_{\eta \rightarrow 0} \mathcal{F}_\eta(v_\eta) \geq \frac{\mu}{2} \int_G |(\partial_x + \partial_y)m_1| + \frac{\beta}{2} \|(\partial_x + \partial_y)m_1\|_{H^{-1}}^2 - \beta\delta^2.$$

At this stage, the arguments in [3] applied to m_1 , entail that

$$\frac{\mu}{2} \int_G |(\partial_x + \partial_y)m_1| + \frac{\beta}{2} \|(\partial_x + \partial_y)m_1\|_{H^{-1}}^2 \geq c_3 \mu^{2/3} \beta^{1/3} \int_G m_1^2 dx,$$

so that, when we combine this with the preceding estimate and the fact that $|m_1| = \frac{1}{\sqrt{2}}$, we obtain

$$\lim_{\eta \rightarrow 0} \mathcal{F}_\eta(v_\eta) \geq c_3 \mu^{2/3} \beta^{1/3} - \beta\delta^2. \quad (4.23)$$

We are now ready to make a choice of δ . Thanks to the assumptions of the theorem, we can choose δ satisfying

$$c_3 \beta^{1/3} \leq \delta^2 < \min\left(\frac{1}{4}, \frac{1}{2} c_3 (\mu\beta)^{2/3}\right). \quad (4.24)$$

Combining (4.21), (4.23) and (4.24) completes the proof of the theorem. \square

Acknowledgements

We would like to thank Robert V. Kohn for several useful comments on an earlier draft of this paper. We thank Felix Otto for pointing out a small error in [5, Figure 2 a] of our previous paper, where the middle zig-zag lines are inverted. The correct figure is Figure 3, making magnetization is divergence free.

The research of R.V was partially supported by the Center for Nonlinear Analysis at Carnegie Mellon University and by the National Science Foundation Grant No. DMS-1411646. The work of RDJ was supported by NSF (DMREF-1629026), and it also benefited from the support of ONR (N00014-18-1-2766), the MURI Program (FA9550-12-1-0458, FA9550-16-1-0566), the RDF Fund of IonE, the Norwegian Centennial Chair Program and the hospitality and support of the Isaac Newton Institute (EPSRC grant EP/R014604/1).

REFERENCES

- [1] Fabrice Bethuel, Haïm Brezis, and Frédéric Hélein. *Ginzburg-Landau vortices*, volume 13 of *Progress in Nonlinear Differential Equations and their Applications*. Birkhäuser Boston, Inc., Boston, MA, 1994.
- [2] Rustum Choksi and Robert V Kohn. Bounds on the micromagnetic energy of a uniaxial ferromagnet. *Communications on pure and applied mathematics*, 51(3):259–289, 1998.
- [3] Rustum Choksi, Robert V Kohn, and Felix Otto. Domain branching in uniaxial ferromagnets: a scaling law for the minimum energy. *Communications in mathematical physics*, 201(1):61–79, 1999.
- [4] Harsh Deep Chopra and Manfred Wuttig. Non-joulian magnetostriction. *Nature*, 521(7552):340–343, 2015.
- [5] Vivekanand Dabade, Raghavendra Venkatraman, and Richard D James. Micromagnetics of galfenol. *Journal of Nonlinear Science*, pages 1–46, 2018.
- [6] Antonio DeSimone and Richard D James. A constrained theory of magnetoelasticity. *Journal of the Mechanics and Physics of Solids*, 50(2):283–320, 2002.
- [7] Antonio DeSimone, Robert V Kohn, Stefan Müller, Felix Otto, et al. Recent analytical developments in micromagnetics. *The science of hysteresis*, 2(4):269–381, 2006.
- [8] Antonio DeSimone, Robert V Kohn, Stefan Müller, Felix Otto, and Rudolf Schäfer. Two-dimensional modelling of soft ferromagnetic films. In *Proceedings of the Royal Society of London A: Mathematical, Physical and Engineering Sciences*, volume 457, pages 2983–2991. The Royal Society, 2001.
- [9] Antonio DeSimone, Stefan Müller, Robert V. Kohn, and Felix Otto. A compactness result in the gradient theory of phase transitions. *Proc. Roy. Soc. Edinburgh Sect. A*, 131(4):833–844, 2001.
- [10] Feng Bo Hang and Fang Hua Lin. Static theory for planar ferromagnets and antiferromagnets. *Acta Math. Sin. (Engl. Ser.)*, 17(4):541–580, 2001.
- [11] Alex Hubert and Rudolf Schäfer. *Magnetic domains: the analysis of magnetic microstructures*. Springer Science & Business Media, 2008.
- [12] Richard D James and Manfred Wuttig. Magnetostriction of martensite. *Philosophical Magazine A*, 77(5):1273–1299, 1998.

- [13] Hans Knüpfer, Robert V Kohn, and Felix Otto. Nucleation barriers for the cubic-to-tetragonal phase transformation. *Communications on pure and applied mathematics*, 66(6):867–904, 2013.
- [14] E Lifshitz. On the magnetic structure of iron. *ZHURNAL EKSPERIMENTALNOI I TEORETICHESKOI FIZIKI*, 15(3):97–107, 1945.
- [15] Joachim A Nitsche. On korn’s second inequality. *RAIRO. Analyse numérique*, 15(3):237–248, 1981.
- [16] M Plancherel and GY Polya. Fonctions entières et intégrales de fourier multiples. *Commentarii mathematici Helvetici*, 10(1):110–163, 1937.
- [17] Ilya Privorotskii. *Thermodynamic theory of domain structures*. Wiley, 1976.
- [18] Elias M Stein and Guido Weiss. *Introduction to Fourier analysis on Euclidean spaces (PMS-32)*, volume 32. Princeton university press, 2016.
- [19] Peter Sternberg. The effect of a singular perturbation on nonconvex variational problems. *Archive for Rational Mechanics and Analysis*, 101(3):209–260, 1988.
- [20] JX Zhang and LQ Chen. Phase-field microelasticity theory and micromagnetic simulations of domain structures in giant magnetostrictive materials. *Acta Materialia*, 53(9):2845–2855, 2005.